

N87-16757

D15-34  
25P  
49631

1986

NASA/ASEE SUMMER FACULTY FELLOWSHIP PROGRAM

MARSHALL SPACE FLIGHT CENTER  
THE UNIVERSITY OF ALABAMA

COMPUTATION OF NOZZLE FLOW FIELDS USING THE  
PARC2D NAVIER-STOKES CODE

Prepared By:	Frank G. Collins, Ph.D.
Academic Rank:	Professor
University and Department:	The University of Tennessee Space Institute
NASA/MSFC:	
Laboratory:	Systems Dynamics
Division:	Aerophysics
Branch:	Unsteady Aerodynamic and Thermal Environment
MSFC Colleague:	Lynn C. Chou
Date:	August 18, 1986
Contract No.:	NGT 01-002-099 The University of Alabama

COMPUTATION OF NOZZLE FLOW FIELDS USING THE  
PARC2D NAVIER-STOKES CODE

by

Frank G. Collins  
Professor of Aerospace Engineering  
The University of Tennessee Space Institute  
Tullahoma, Tennessee

ABSTRACT

Supersonic nozzles which operate at low Reynolds numbers and have large expansion ratios have very thick boundary layers at their exit. This leads to a very strong viscous/inviscid interaction upon the flow within the nozzle and the traditional nozzle design techniques which correct the inviscid core with a boundary layer displacement do not accurately predict the nozzle exit conditions. In addition, if the nozzle exit density becomes low enough rarefaction effects in the form of velocity slip and temperature jump at the wall must be accounted for.

The present work used a full Navier-Stokes code (PARC2D) to compute the nozzle flow field. Grids were generated using the interactive grid generator code TBGG. All computations were made on the NASA MSFC CRAY X-MP computer. Comparison was made between the computations and in-house wall pressure measurements for CO<sub>2</sub> flow through a conical nozzle having an area ratio of 40. Satisfactory agreement existed between the computations and measurements for a stagnation pressure of 29.4 psia and stagnation temperature of 1060 °R. However, agreement did not exist at a stagnation pressure of 7.4 psia. Several reasons for the lack of agreement are possible. The computational code assumed a constant gas gamma whereas gamma for CO<sub>2</sub> varied from 1.22 in the plenum chamber to 1.38 at the nozzle exit. The computations were performed assuming adiabatic, no-slip walls, both of which may not be correct. Finally, it is possible that condensation occurred during the expansion at the lower stagnation pressure. The next phase of the work will incorporate variable gamma and slip wall boundary conditions in the computational code.

### ACKNOWLEDGEMENTS

I wish to thank Dr. Lynn Chou for the opportunity to work with him during the past two summers. The experience has been stimulating and professionally rewarding and has allowed me to get into an area of research that I otherwise would have been unable to enter. I also wish to acknowledge the hospitality of Mr. Werner Dahm, Division Chief and Dr. Terry Greenwood, Branch Chief, for the past two summers.

The work described in this report could not have been accomplished without the assistance of many persons whom I would like to thank. These include Young-Ching Lee, Edwin Brewer and Dennis Goode at NASA MSFC and Kyle Cooper, William Phares and David Huddleston at Sverdrup Technology, Inc., AEDC Group. Their assistance was essential for the completion of this work.

## INTRODUCTION

Low Reynolds number, large expansion ratio, and supersonic nozzles are frequently used for control of spacecraft. An accurate knowledge of their thrust is required for designing the spacecraft control system. Recently the contamination to the spacecraft from the nozzle exhaust has become a concern and accurate computations of the exhaust plume have been required. The flow in such nozzles possesses strong viscous/inviscid interactions at their exit due to the thick boundary layers. Traditional nozzle design techniques, such as the use of the method of characteristics to calculate the inviscid core and boundary layer theory to compute the displacement thickness, fail to predict the strength of the viscous/inviscid interaction. Therefore, it is necessary to use a full Navier-Stokes code for this purpose.

The present work used an existing code that incorporates the full Navier-Stokes equations and viscous stress terms to calculate the flow fields within a conical nozzle having an area ratio of 40. Comparison was made with in-house measurements that had been performed on this nozzle using CO<sub>2</sub> as the gas. Tests were performed at several stagnation pressure levels, the lowest resulting in a exit wall Knudsen number of 0.06. Under these conditions slip flow conditions could be expected to exist at the nozzle exit. This presents an additional complication to the computation of the flow field. The PARC2D code, developed by Sverdrup Technology, Inc., AEDC Group (ref. 6) has demonstrated the ability to calculate such nozzle flow fields and their plumes. The slip flow could be included as a new boundary condition subroutine within the program. Therefore, it was chosen to perform this task.

## OBJECTIVES

The objectives of this work were to:

- 1) generate a computational grid using the interactive program TBGG on the MSFC VAX 785 computer,
- 2) modify the output file from TBGG and generate additional input files for PARC2D, copy them to a tape and transfer the files to the EADS system,
- 3) install and make operational on the MSFC CRAY machine the Navier-Stokes code PARC2D,
- 4) couple the grid generator output file to the PARC2D code,
- 5) run PARC2D for conditions that matched those of in-house measurements of CO<sub>2</sub> flow through a 40:1 area ratio nozzle
  - a) determine how to converge the program solution,
  - b) compare the computed results with the measurements as the value of gamma was varied,
  - c) compare the computed results and measurements as the grid and downstream boundary condition were varied,
- 6) learn how to modify PARC2D to include slip wall boundary conditions,
- 7) learn how to run PARC2D to obtain the nozzle plume flow field and to calculate the force on a nozzle end plate.

## GRID GENERATION

The first step to calculating the flow in a nozzle is to generate an appropriate computational grid. Two grid generator programs acquired from Arnold Engineering Development Center were placed on the MSFC CRAY machine but some of the routines were found to be incompatible with the IBM front end and, rather than rewrite these portions of the programs, it was decided to use a grid generator that had previously been installed on the VAX system.

The grid generator that was used is called TBGG and was developed by Smith and Wiese at Langley Research Center (ref. 1). It is interactive in the 4010 mode and can be used to generate body-fitted grids algebraically. The number of grid points can be changed, with the maximum possible number controlled by a parameter IPX. This number was initially 100 but was later changed to 200. The program starts from a RESTART file that had been previously created (for given geometry) or from a file DATANEW that is created and contains a listing of the boundary coordinates. The grid lines can be concentrated at different regions of the flow field using several functions. For the nozzle flow fields the bi-exponential function was used for the top and bottom surfaces and the connecting curve. TBGG generates two output files, RESTART, which is an unformatted file that can be used to start the program next time, and GRIDOUT, which is a formatted output file. A modification of this latter file was used as part of the necessary input to the Navier-Stokes code.

Computations were performed on a nozzle configuration that was used for MSFC in-house measurements, using CO<sub>2</sub> as the gas. The major geometric parameters for the nozzle and upstream plenum chamber are shown in Figure 1. This geometry was introduced into TBGG as a discrete number of dimensional points. The bi-exponential function was used to cluster the grids perpendicular to the nozzle axis (x-axis in Figure 2) in the region of the nozzle throat by choosing  $K_1 = 0.57$  and  $K_2 = -2.0$  for both top and bottom curves (see ref. 1). For the connecting curve  $K_1 = 0.50$  and  $K_2 = 2.0$  were chosen to place the grid points near the nozzle walls and symmetrically about the centerline (Figure 3). Because the Navier-Stokes code only required grid points from the centerline to the wall, 99 grid points

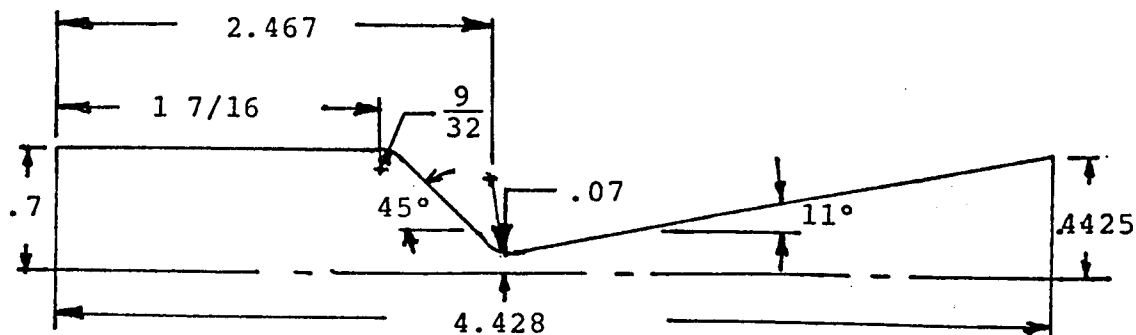


Figure 1. Geometry of conical nozzle and plenum chamber. All dimensions are in inches.  
 $A_e/A_* = 40$ .

were chosen in the y-direction to place one on the centerline and 100 were chosen in the x-direction. Enlargements of the grid next to the wall in the throat region and at the nozzle exit are shown in Figures 4 and 5, respectively.

The output file GRIDOUT gave the arrays  $[(X(J, K), K=1, KMAX), J=1, JMAX]$  and the same for  $Y(J, K)$ , where  $J$  is the grid index in the x-direction ( $JMAX = 100$ ) and  $K$  is the index in the y-direction ( $KMAX = 99$ ). As stated above, the Navier-Stokes code required grid points only from the nozzle centerline to one wall and it required that they be ordered in the opposite fashion. Thus, the code required  $[(X(J, K), J=1, JMAX), K=1, KMAX]$  where now  $KMAX$  was 50. A program was written to accomplish this plus generate the other necessary input arrays (see next section). This file was copied to magnetic tape and read onto the EADS system.

The grid just described was discovered to be inadequate (see next section). Therefore, a second grid was generated using the geometry shown in Figure 6. This geometry contained one inch less plenum chamber, which was added as an exhaust chamber downstream of the nozzle exit. It was also decided to increase the number of grid points to 200 x 199. This required changing the parameter statement, as

ORIGINAL PAGE IS  
OF POOR QUALITY

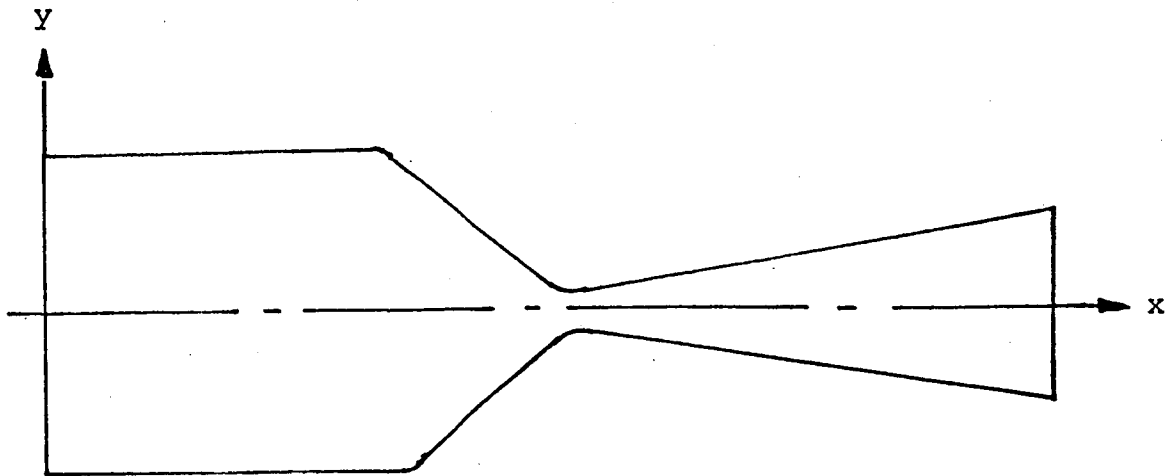


Figure 2. Schematic of geometry used for 100 x 99 grid. All  $(x,y)$  coordinates are defined with respect to this geometry.

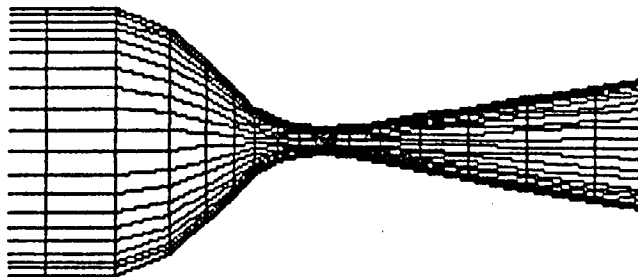


Figure 3. Portion of 20 x 20 grid applied to geometry above, illustrating the concentration of grid lines at outer walls and nozzle throat.



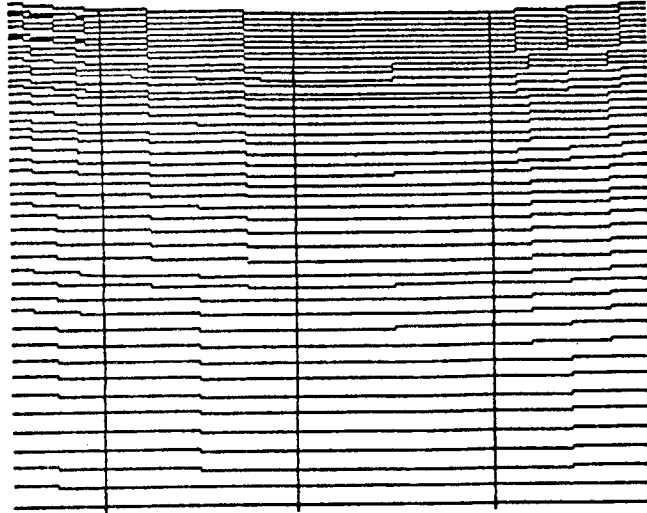
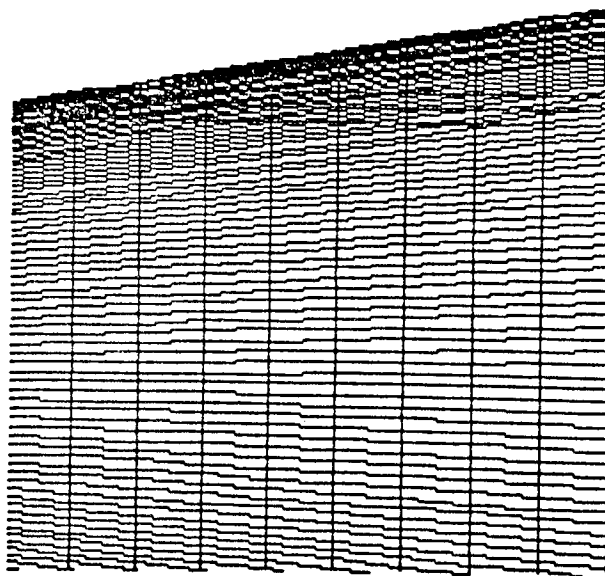


Figure 4. Blow-up of 100 x 99 grid in nozzle throat region.



ORIGINAL PAGE IS  
OF POOR QUALITY

Figure 5. Blow-up of 100 x 99 grid next to nozzle wall at exit plane.

ORIGINAL PAGE IS  
OF POOR QUALITY

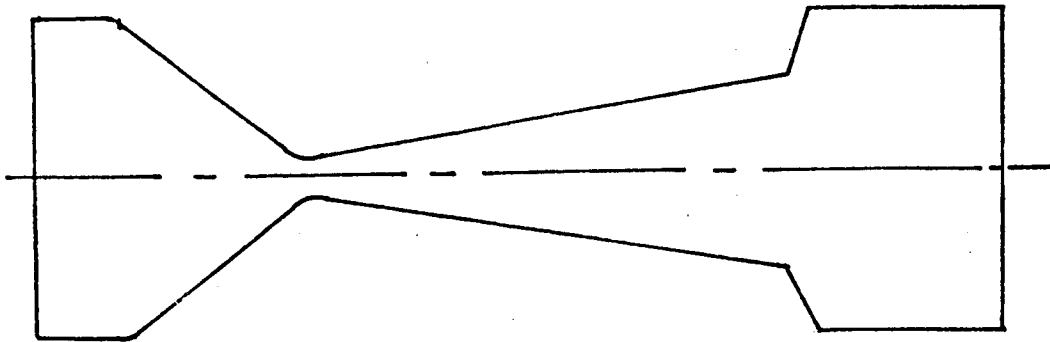


Figure 6. Schematic of geometry used for 200 x 199 grid, with nozzle exiting into a tube.

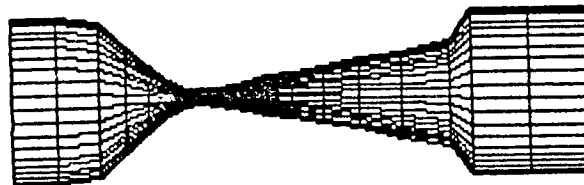


Figure 7. 20 x 20 grid applied to geometry above, illustrating concentration of grid lines at the outer walls and nozzle throat.

stated earlier. Again the grids lines were concentrated near the nozzle throat with  $K_1 = 0.33$ ,  $K_2 = -2.0$  and near the walls with  $K_1 = 0.50$ ,  $K_2 = 2.0$  (Figure 7). Problems arose when trying to get a useful grid that would flow from the nozzle into the exhaust chamber. A perpendicular end plate failed to give continuity to the grid lines (Figure 8) and since it was desirable to have one set of grid lines perpendicular to the nozzle axis (to be able to plot properties across a nozzle section) a 1/16 inch radius connecting the nozzle exit with a perpendicular end plate was also unsatisfactory (Figure 9). However, adding a slope to the end plate did yield a useful grid (Figure 10). This grid, modified to 200 x 100, was the one that was used for the latter calculations.

#### NAVIER-STOKES COMPUTATIONAL CODE

The Navier-Stokes code, PARC2D, is a modification of the ARC2D code that was developed by Pulliam and Steger at NASA Ames. Space does not permit more than a cursory description of that code but more details are given in references 2 to 4. It uses a thin layer approximation to the Navier-Stokes equations with parabolized viscous stress terms. It is written in strong conservative form in curvilinear coordinates, utilizing the delta form (ref. 7). The noniterative implicit approximate factorization scheme of Beam and Warming (ref. 5) is used with fourth order artificial dissipation.

The PARC2D code is a modification of the ARC2D code by Sverdrup Technology, Inc., AEDC Group which removed the thin layer approximation and the approximate stress terms (ref. 6). It is fully elliptic, requiring closed boundary conditions and an initial condition everywhere in the flow field. The code is modular and fully vectorized. It assumes that the gas is a perfect gas with constant gamma and Prandtl number but uses the Sutherland viscosity law for the temperature variation of viscosity. An initial test over 400 iterations indicated that the vectorization decreased the CPU time on the MSFC EADS system by a factor of 5.22.

Some of the important required input quantities to the code are listed in Table I. The Reynolds number is based upon a reference sound speed and length. For the present calculations the stagnation conditions were taken as reference and the reference length was one inch, since the grid

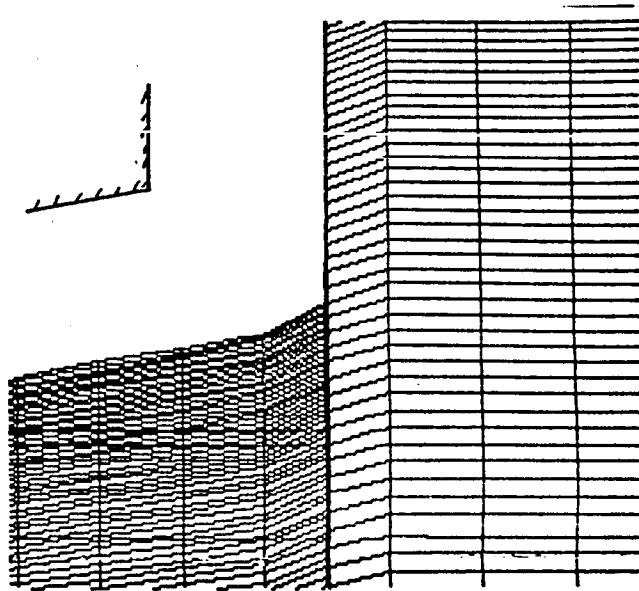


Figure 8. Detail of 200 x 199 grid at nozzle exit with end plate at 90° to nozzle centerline.

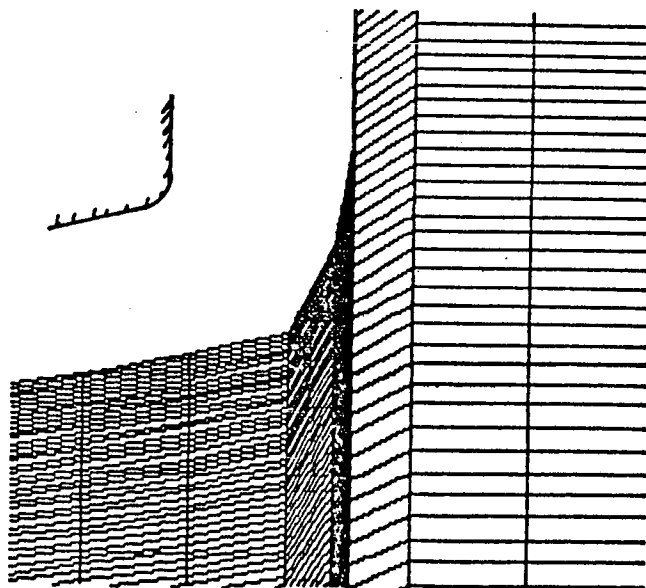


Figure 9. Detail of 200 x 199 grid at nozzle exit with 1/16 inch radius fillet between the nozzle exit and 90° end plate.

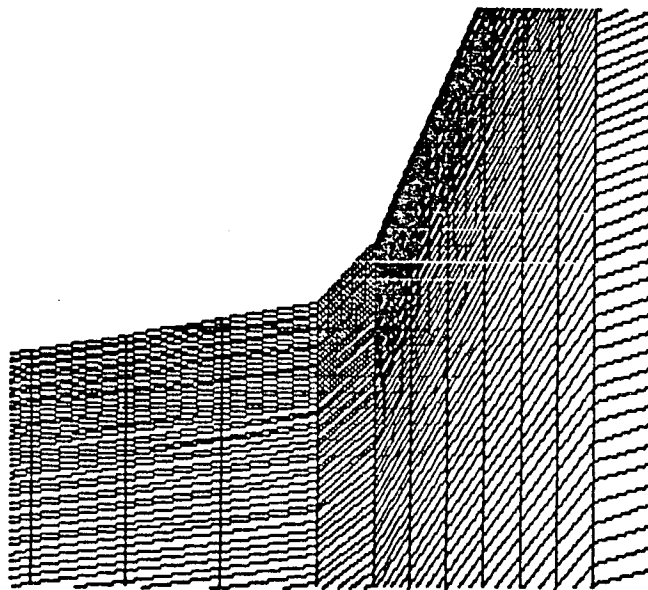
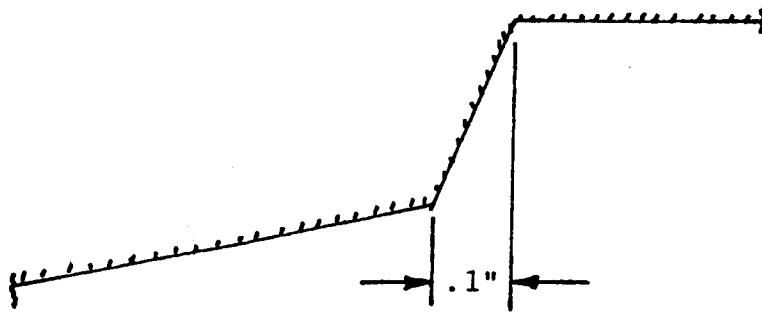


Figure 10. Detail of 200 x 199 grid at nozzle exit with sloping end plate as detailed above.

TABLE I

OPERATIONAL ASPECTS OF PARC2D

Nondimensionalization:  $\bar{q} = q/a_r$ ;  $\bar{p} = p/\gamma p_r$ ;  $\bar{\rho} = \rho/\rho_r$

$$\bar{E} = \frac{\bar{p}}{\gamma-1} + \frac{1}{2} \bar{\rho} \bar{q}^2; \quad Re = \frac{\rho_r a_r L}{\mu_r}$$

$q$  = speed,  $a$  = sound speed,

$( )_r$  = reference

Namelist inputs:

$\gamma$ ,  $Re$ , Prandtl number,  $P_r$ ,  $T_r$ ,  
 $J_{max}$ ,  $K_{max}$  selection from adia-  
 batic/constant wall temperature,  
 viscous/inviscid, axisymmetric/  
 two-dimensional, laminar/  
 turbulent

Initial condition input: Iteration number, gamma  
 arrays  $X(J, K)$ ,  $Y(J, K)$ ,  $\rho(J, K)$ ,  
 $\rho u(J, K)$ ,  $\rho v(J, K)$ ,  $E(J, K)$

coordinates were calculated in inches. Although several different conditions were used as initial conditions it was found that the fastest convergence occurred by taking  $u = v = 0$  and  $\bar{p}$  and  $\bar{E}$  equal to their stagnation values, i.e.,  $\bar{p} = 1$ ,  $\bar{E} = 1/\gamma(\gamma-1)$ . These values were assigned initially throughout the flow field. Other options used are as follows: adiabatic wall, axisymmetric, viscous, laminar. Free boundaries (allowing inflow or outflow) were assumed at the upstream and downstream boundaries in Figures 2 and 6, and the other boundaries were axis of symmetry and no slip/adiabatic wall. It would have been possible to have taken the upper and lower portions of the chamber downstream of the nozzle in Figure 6 as outflow boundaries also but that was not done. A parameter statement for NX, NY and NM had to be changed to allow JMAX = 200. Note that NM must be at least as large as the largest of the other two parameters.

Boundary conditions must be imposed upon all of the boundaries. For the free boundaries this consists of a specification of the pressure. The stagnation pressure was imposed upstream but the downstream boundary condition posed a problem. For flows with strong viscous/inviscid interaction the pressure cannot be expected to be constant across even a contoured nozzle and even greater pressure variations would exit across the exit of a conical nozzle. However, a constant downstream pressure must be specified. It is usually prudent to specify a pressure somewhat lower than the minimum expected downstream pressure. No boundary conditions are required on the axis nor on the wall. If constant temperature wall conditions are assumed then the temperature must be specified. Note that the entire wall does not have to be assumed to be at the same temperature.

Placing the downstream boundary conditions at the nozzle exit plane produced unacceptable stagnation pressure fluctuations on the centerline upstream at the exit (Figure 11). It was for this reason that the second geometry (Figure 6) was used for the latter calculations. The boundary condition, however, had only a small effect upon the other results, such as the exit Mach number, as can be seen from the two calculations given in Table II for  $\gamma = 1.33$  and  $p_0 = 29.4$  psia. These two Mach numbers differ by only 0.3 percent.

An efficient convergence procedure for these nozzle problems was discovered. The steps are as follows:

- 1) Initially set  $q = 0$ ,  $\bar{p} = 1$  and  $\bar{E} = 1/\gamma(\gamma-1)$  everywhere in flow field.

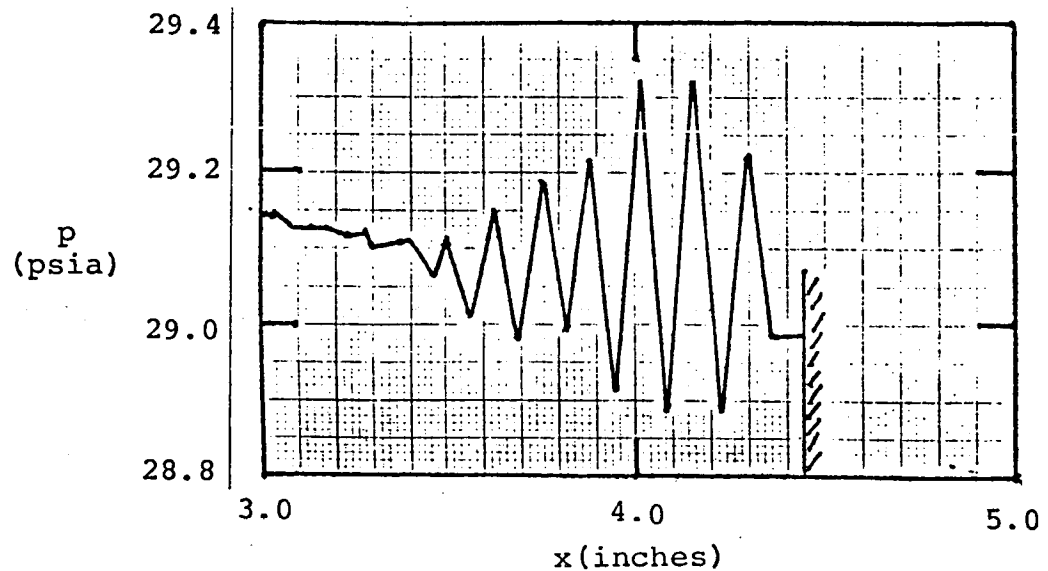


Figure 11. Centerline stagnation pressure approaching the exit plane.  $p_o = 29.4$  psia,  $T_o = 1060$  °R,  $\gamma = 1.3$ ,  $Re = 68,115$ ,  $100 \times 50$  grid.

- 2) Set initial parameters as follows:  $DIS2 = 0.2$ ,  $DIS4 = 0.35$ ,  $PCQMAX = 10.0$ ,  $DTCAP = 5.0$ . Run until the axial velocity is positive everywhere in the plenum chamber.
- 3) Slowly reduce  $DIS4$  to 0.25 (all other parameters constant).
- 4) Slowly reduce  $DIS2$  to 0.00.
- 5) Check  $DT$  and set  $DTCAP$  to about one-half of the minimum  $DT$  for the last series of iterations. Then run until  $L2$  reaches an acceptable value ( $10^{-8}$  to  $10^{-9}$ ).

In this discussion  $DIS4$  and  $DIS2$  are parameters related to the fourth order and second order dissipation, respectively,  $PCQMAX$  sets the maximum change in any variable during an iteration,  $DT$  is the time step and  $DTCAP$  is the maximum allowable time step.  $L2$  is a convergence measure.



Convergence is also improved by minimizing the amount of plenum chamber that is included in the computational domain. Small disturbances in this low velocity region damp very slowly.

## RESULTS

Computations were made using the test conditions that corresponded to the MSFC in-house measurements on the nozzle described in Figure 1. The test gas was  $\text{CO}_2$ , stagnation temperature was 1060 °R and the stagnation pressure had two values, 29.4 and 7.4 psia. Since only wall pressure measurements were made, that was the only parameter that could be used for comparison with the computations. The computational code assumed a constant gamma whereas the gamma for  $\text{CO}_2$  varied from about 1.22 in the plenum chamber to 1.38 at the exit. Therefore, exact comparison could never be expected to occur between the measurements and computations.

A summary of some of the results is given in Table II. Many of the initial computations were performed at an erroneous Reynolds number but their results are included for completeness. Comparison of computed and measured wall pressures is given in Figure 12. The agreement at the higher stagnation pressure is very good (also see Figure 13 which is drawn to magnify the differences) and could be improved by increasing the assumed value of  $\gamma$ .

The effect of  $\gamma$  on the results is shown by the two computed results at the lower pressure. The  $\gamma = 1.33$  computations compare more favorably with the measurements than do those at  $\gamma = 1.30$  but the agreement is still not good. Several reasons are possible for the lack of agreement, in addition to the need for a variable  $\gamma$  computational code. These include the possibility that the adiabatic wall boundary condition is not applicable and computations at a constant wall temperature should be performed to examine that possibility. In addition, there is a strong possibility that condensation of the  $\text{CO}_2$  was occurring during the expansion and agreement would not be expected until the stagnation temperature was raised to eliminate all possibility for condensation. Finally, at the exit the Knudsen number is about 0.06, based on a mean free path at wall conditions

and a crude estimate of the displacement thickness. Slip is expected to occur under such circumstances and the slip wall boundary condition formulated by the author (ref. 8) should be implemented rather than the no-slip condition.

Typical profiles of Mach number and static temperature across the nozzle at a location near the nozzle exit are shown in Figure 14. The large temperature gradients near the wall are caused by the assumed adiabatic wall condition.

Very large wall pressure gradients were observed at the nozzle exit. For the original grid, Figure 2, this influence extended upstream several grid points in the subsonic boundary layer. This was caused by the requirement of the code to exactly match the prescribed downstream boundary pressure at the wall and was one of the reasons for going to the configuration shown in Figure 6. However, a rapid expansion still existed right at the exit because of the details of the grid that was generated (Figure 10). In this case the expansion only occurred over the last grid point. This problem can be eliminated by slightly extending the nozzle and using the computed properties only up to the actual nozzle exit plane.

The usefulness of the computational results can be greatly enhanced by the implementation of plotting facilities that are part of the EADS system and then Mach number contours, for example, can be drawn for the entire nozzle.

TABLE II

SUMMARY OF RESULTS  
(Adiabatic wall)

Convergence information:  $p_o = 29.4$  psia

$\gamma$	Re	Grid	Number Iterations	$L^2$	CPU Time
1.4	70,686	100 x 50	23,000	$4.5 \times 10^{-9}$	40 min
1.3	664,341	200 x 100	9,500	$3.3 \times 10^{-9}$	64 min

Exit properties at centerline:

$p_o$ (psia)	$\gamma$	Re	Grid	Centerline Mach Number
29.4	1.30	68,115	100 x 50	4.295
	1.33	68,896		4.409
	1.40	70,686		4.724
	1.33	68,896	200 x 100	4.395
	1.31	666,891		4.652
7.4	1.40	17,792	100 x 50	4.188
	1.30	168,496	200 x 100	4.454
	1.33	170,429		4.601
	1.40	174,856		4.967
	1.33	170,429		4.671

ORIGINAL PAGE IS  
OF POOR QUALITY

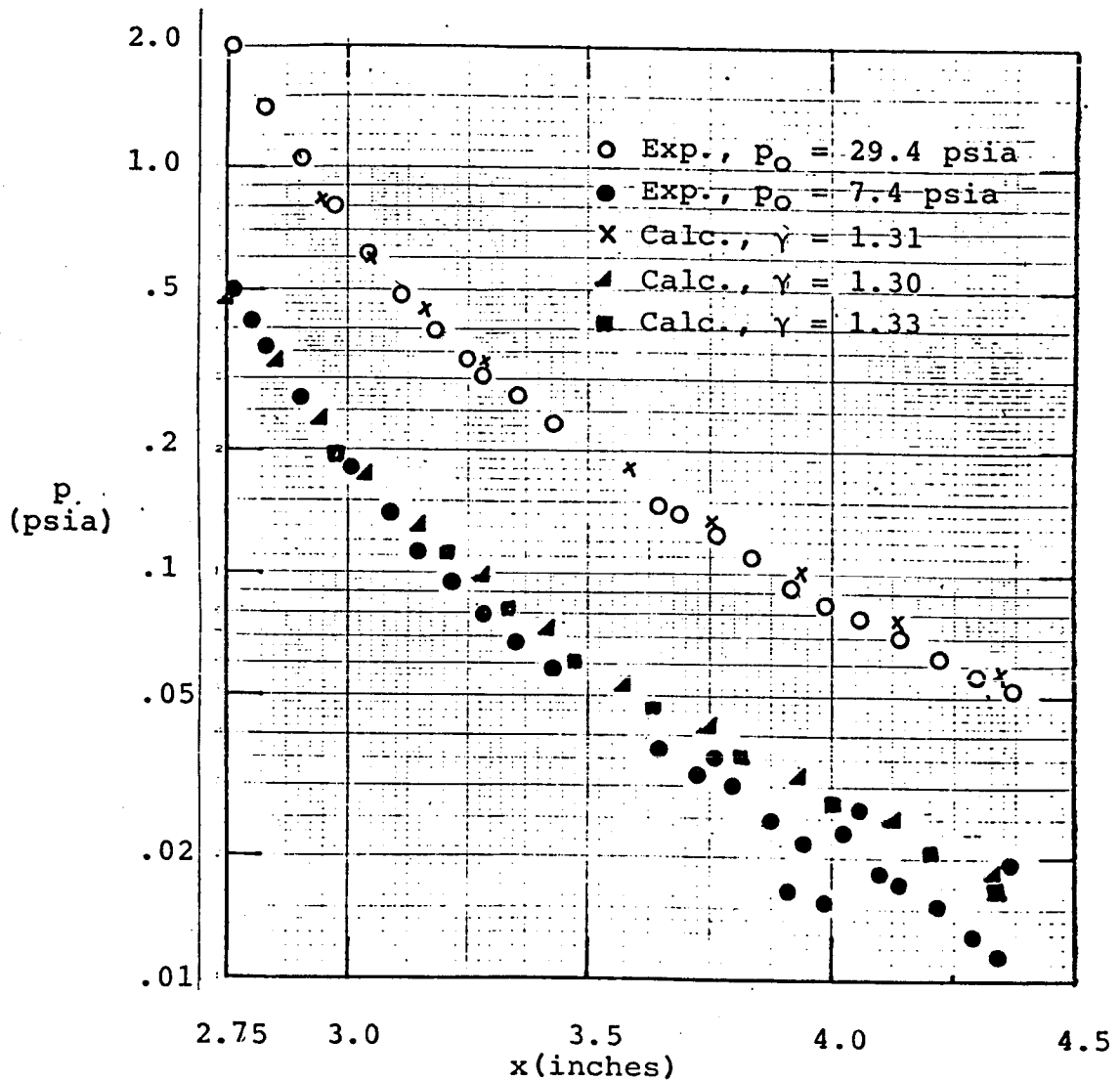


Figure 12. Comparison of measured and computed nozzle wall pressure distributions. Computations used 200 x 100 grid.  $T_0 = 1060$  °R.

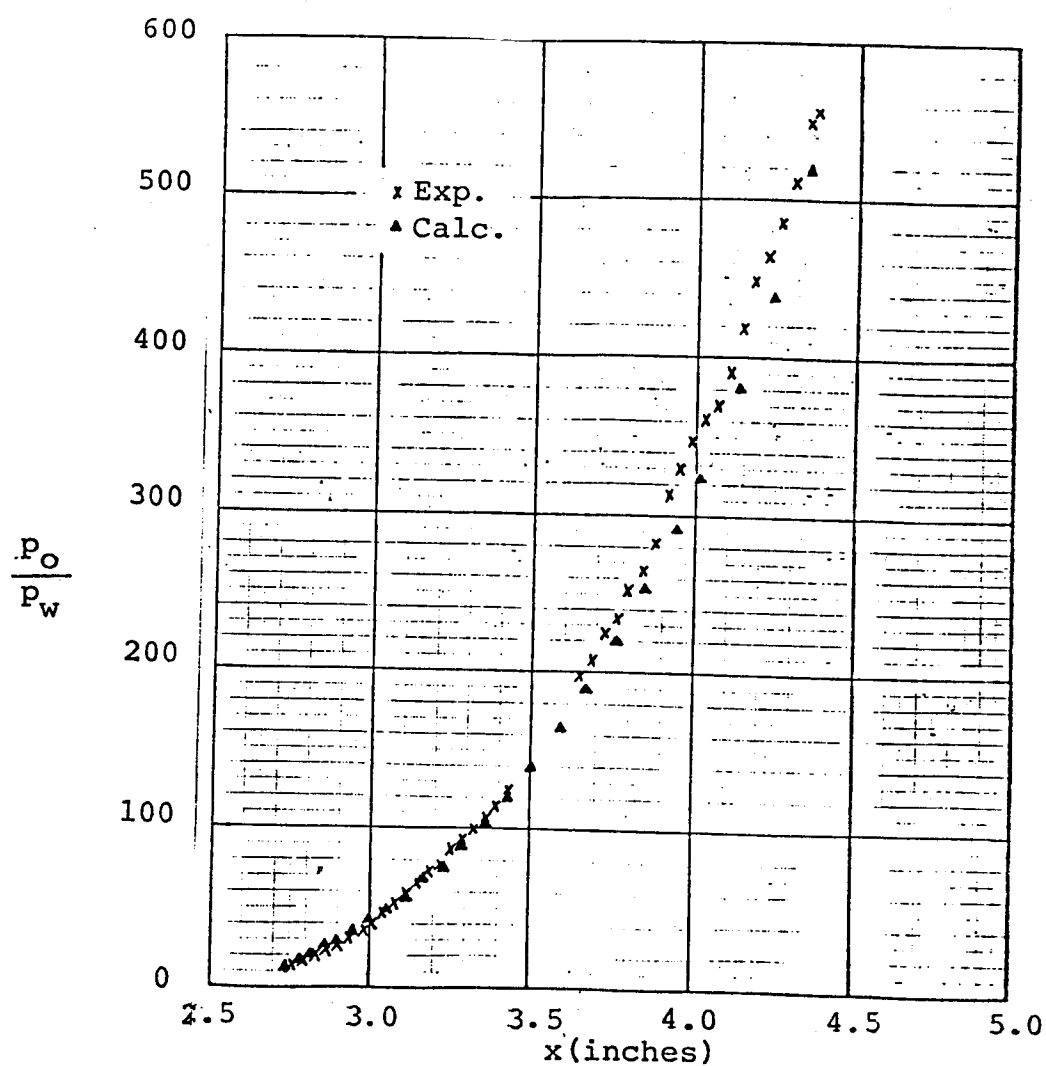


Figure 13. Comparison of measured (CO<sub>2</sub>) and computed nozzle wall pressures.  $p_o = 29.4$  psia,  $T_o = 1060$  °R. Calculations used  $\gamma = 1.31$  and  $200 \times 100$  grid.

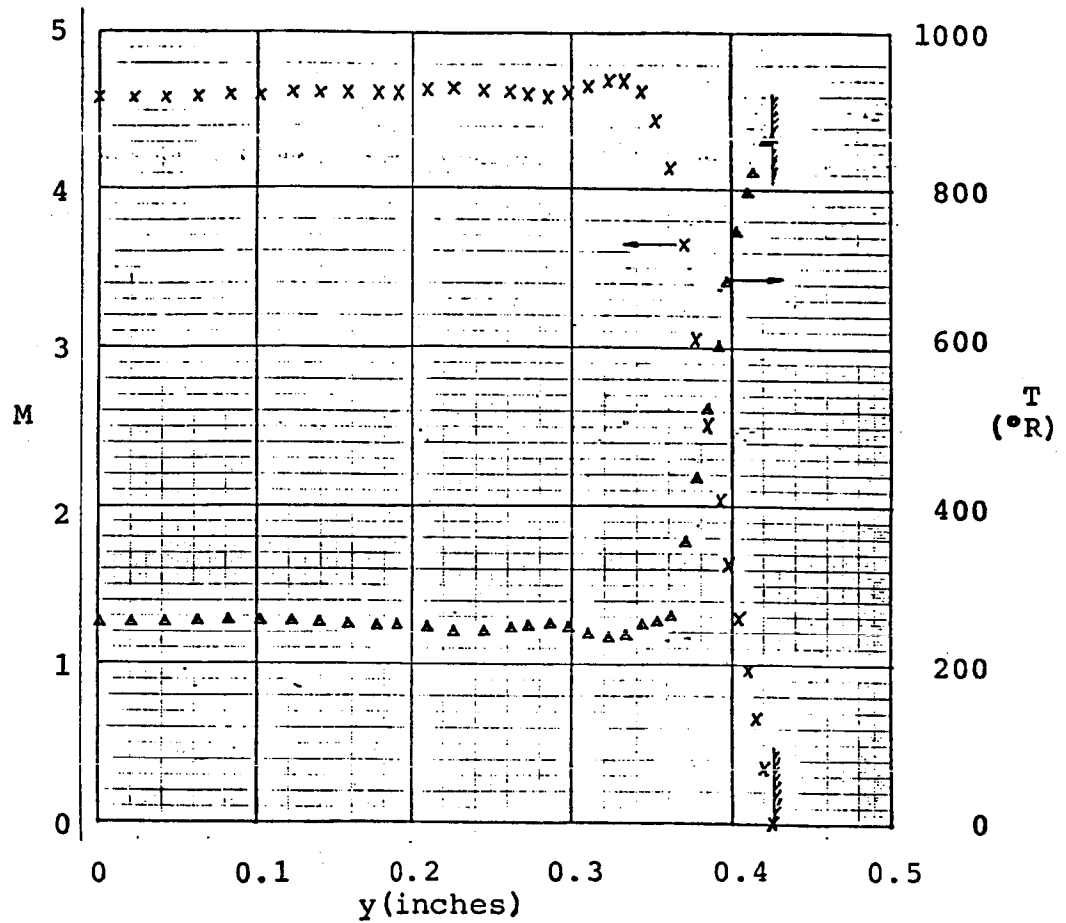


Figure 14. Computed Mach number and static temperature profiles across the nozzle at  $x = 4.342$  inches.  $p_0 = 29.4$  psia,  $T_0 = 1060$  °R,  $\gamma = 1.31$ ,  $Re = 666,891$ , adiabatic wall.

## CONCLUSIONS AND RECOMMENDATIONS

The following conclusions can be made from results of this study.

- 1) The grid generator code TBGG provided a good means generating useful computational grids for the Navier-Stokes computations of the nozzle flow. However, it had several drawbacks. First, it was inconvenient to have to generate the grid on the VAX, transfer it to a tape and place it on the CRAY. Second, it was difficult to concentrate the grid points in all of the regions of interest. Finally, it would be difficult to use this grid generator for more complicated geometries and grid generators that can patch various regions together are available for such circumstances.
- 2) The PARC2D code yields accurate solutions for the flow field in supersonic nozzles at low Reynolds numbers where large viscous/inviscid interaction exists. Because the code is modular it can be easily modified. An efficient convergence procedure was developed for these nozzle flows. The amount of plenum chamber included in the computation should be minimized and an exhaust chamber should be provided downstream of the nozzle exit to increase the accuracy and minimize the number of iterations.

A number of recommendations for additional work or improvements to the code can be made.

- 1) The constant gamma restriction to the PARC2D code should be removed. Sverdrup Technology, Inc., AEDC Group, is presently modifying the code to accommodate variable gamma.
- 2) Additional computations should be made at other values of gamma, especially for the low stagnation pressure test, to see if improved agreement of the computations with the measurements could not be achieved. Computations should also be performed at constant wall temperature rather than an adiabatic wall to see the influence of that boundary condition upon the flow.

- 3) Subroutines should be written to calculate boundary layer thicknesses, etc., to allow comparison with other computational techniques.
- 4) The plotting routines available on the CRAY system should be utilized to better understand the nature of the solutions that have been obtained.
- 5) Objectives numbers 6) and 7) were not accomplished due to lack of time. These should be implemented, especially the slip boundary condition. That condition will be required, along with the variable gamma, before the computations will satisfactorily agree with the measurements at the lowest stagnation pressure. Also, flow should be allowed to leave the sides of the downstream region to more accurately model the nozzle plume.



## REFERENCES

1. Smith, R. E. and Wiese, M. R., "Interactive Algebraic Grid-Generation Technique", NASA TP 2533, 1986.
2. Steger, J. L., "Implicit Finite-Difference Simulation of Flow About Arbitrary Geometries with Application to Airfoils", AIAA Paper No. 77-665, 1977.
3. Pulliam, T. H. and Steger, J. L., "Implicit Finite-Difference Simulations of Three-Dimensional Compressible Flow", AIAA J. 18, 159 (1980).
4. Pulliam, T. H. and Steger, J. L., "Recent Improvements in Efficiency, Accuracy and Convergence for Implicit Approximate Factorization Algorithm", AIAA-85-0360, 1985.
5. Beam, R. M. and Warming, R. F., "An Implicit Factored Scheme for the Compressible Navier-Stokes Equations", AIAA J. 16, 393 (1978).
6. Cooper, G. K., "Development and Application of a General Purpose Navier-Stokes Code", presented at the First World Congress on Computational Mechanics, Austin, Texas, September 1986.
7. Anderson, D. A., Tannehill, J. C. and Pletcher, R. H., Computational Fluid Mechanics and Heat Transfer, Hemisphere Publishing Corporation, New York, 1984.
8. Collins, F. G., "Low Density Gas Dynamic Wall Boundary Conditions", NASA CR-178709, January 1982.